Sustainable Food Technology

ROYAL SOCIETY OF CHEMISTRY

PAPER

View Article Online
View Journal | View Issue

Cite this: *Sustainable Food Technol.*, 2025, **3**, 470

Green active food packaging films based on nanocomposites of PHBV/sepiolite/essential oils†

Renata Cerruti da Costa, [a] Pâmela Rosa Oliveira, [a] Leandro Guarezi Nandi, [b] Daiane Mara Bobermin, [c] Marília Miotto, [d] Ismael Casagrande Bellettini, [a] Janaina da Silva Crespo, [e] Tales da Silva Daitx, [f] Cristiano da Silva Teixeira [a] and Larissa Nardini Carli *[a]

One of the cutting-edge strategies for food packaging is the use of an active storage system, also known as active packaging. In this context, this work aims to evaluate the chemical, physical, and microbiological properties of active poly(hydroxybutyrate-*co*-hydroxyvalerate)/sepiolite nanocomposite films for application in antibacterial food packaging. In these nanocomposite films, three essential oils (EOs) (oregano – OEO, rosemary – REO, and basil – BEO) with different active compounds were incorporated and their effects were compared. The clay mineral added to the nanocomposites acted as a nucleating agent and enhanced the degree of crystallinity of PHBV, without compromising the thermal stability of the compositions. The EOs exhibited a plasticizing effect on the PHBV matrix with a decrease in the glass transition temperature and elastic modulus, varying according to the type of EO. A slow and controlled release of the EOs under simulated food conditions was also noted, especially for films containing OEO, which was related to the good dispersion of sepiolite nanoparticles in the PHBV matrix that resulted from a combined effect of the clay mineral and OEO. The obtained films exhibited satisfactory antibacterial effects against *S. aureus* and *E. coli* bacteria, with a log reduction of more than 2 log cycles. *In situ* tests in commercial mozzarella cheese for 30 days in the presence of *E. coli* and *L. monocytogenes* revealed a lower microbiological count for active films compared to the control film, evidencing the potential of these nanocomposites for application as active packaging in guaranteeing product safety.

Received 31st July 2024
Accepted 24th December 2024

DOI: 10.1039/d4fb00232f

rsc.li/susfoodtech

Sustainability spotlight

The development of functional packaging is a forthcoming strategy towards the guarantee of the quality of food. Due to the environmental concerns caused by conventional polymers from the fossil-fuel origin, the use of biodegradable polymers and polymers from renewable sources for this application arises as a promising strategy. Furthermore, the use of additives entirely from renewable resources, guaranteeing the complete life cycle of the material, meets the principles of circular economy. The incorporation of essential oils results in an active packaging with antibacterial properties. The synergistic effect of the essential oils with the clay nanoparticles provides a control over the release rate of active agents into the packaging system, thus extending the effect of the active compound and increasing the shelf life of the food.

1 Introduction

In the modern world, the main purpose of food packaging is the protection and preservation of products, prevention of damage that occurs during transportation, as well as the loss of integrity by external factors such as oxygen, humidity, ultraviolet radiation, and microorganisms. Additionally, it can be a vehicle for consumer information.[1] In this scenario, various efforts have

[a]*Centro Tecnológico de Ciências Exatas e Educação (CTE), Universidade Federal de Santa Catarina, Rua Engenheiro Udo Deeke, 485 Blumenau, 89065-100, SC, Brazil. E-mail: renatadrc@gmail.com; pamela.rosa@posgrad.ufsc.br; ismael.bellettini@ufsc.br; c.teixeira@ufsc.br; larissa.carli@ufsc.br; Fax: +55 47 3232 5187; Tel: +55 47 3232 5187*

[b]*Departamento de Engenharia Química e Engenharia de Alimentos, Universidade Federal de Santa Catarina, R. do Biotério Central, s/n, Florianópolis, 88037-010, SC, Brazil. E-mail: guarezi.nandi@ufsc.br*

[c]*Departamento de Farmacologia, Universidade Federal de Santa Catarina, R. João Pio Duarte Silva, s/n, Florianópolis, 88037-000, SC, Brazil. E-mail: daiane.bobermin@ufsc.br*

[d]*Departamento de Ciência e Tecnologia de Alimentos, Universidade Federal de Santa Catarina, Rod. Admar Gonzaga, 1346, Florianópolis, 88034-000, SC, Brazil. E-mail: marilia.miotto@ufsc.br*

[e]*Universidade de Caxias do Sul, Área do Conhecimento de Ciências Exatas e Engenharias, Rua Francisco Getúlio Vargas, 1130, Caxias do Sul, 95070-560, RS, Brazil. E-mail: jscrespo@ucs.br*

[f]*Instituto de Química, Universidade Federal do Rio Grande do Sul, Av. Bento Gonçalves, 9500, Porto Alegre, 91501-970, RS, Brazil. E-mail: tales.daitx@ufrgs.br*

† Electronic supplementary information (ESI) available. See DOI: https://doi.org/10.1039/d4fb00232f

been taken recently in order to produce packaging materials with novel functionalities, which leads to active food packaging that contains active compounds that prevent contamination or degradation of food, thus extending its shelf life. The most researched system is formed by the incorporation of antimicrobial or antioxidant substances that can act on the surface of the food by direct contact or in the headspace between the packaging and the food by indirect contact. These mechanisms prevent the growth of microorganisms and/or food spoilage.[1]

A promising approach is the use of essential oils (EOs), which are natural preservatives found in various plant components including bark, stems, roots, flowers, and fruits, and are generally recognized as safe (GRAS) by the Food and Drug Administration (FDA).[2] Several herbs and spices contain EOs and exhibit antimicrobial activity, such as rosemary, oregano, thyme, and mint.[3] Approximately 90–95% of the composition of EOs comprises volatile compounds, with the major compounds responsible for antimicrobial activity being aldehydes, phenols, and oxygenated terpenoids,[4] with their composition varying according to the plant features and geographical characteristics.[5] The mechanisms of action of EOs are not yet fully understood, but include changes in the permeability and damage to the cell membrane due to the hydrophobic characteristic of their structures, the penetration of active compounds into the bacterial cell, and the inhibition of their functional properties, both in Gram-positive and Gram-negative bacteria.[2,5–7]

Conventional non-biodegradable plastics such as polyethylene (PE), polyethylene terephthalate (PET), and polyvinyl chloride (PVC) are often used for food packaging application.[1,8] However, their fossil-fuel origin and end-of-life scenario have led to detrimental effects on the environment, including slow degradation rates that vary from tens to thousands of years, increased greenhouse gas emissions and microplastics pollution.[1,9,10] Since the choice of suitable plastics should rely on environmental concerns, one way to mitigate those problems is to replace these materials with polymers that are obtained from renewable sources and/or are biodegradable. Among them, biodegradable polymers such as poly(lactic acid) (PLA),[11] poly(butylene adipate-*co*-terephthalate) (PBAT),[12] and poly(hydroxybutyrate-*co*-hydroxyvalerate) (PHBV)[13] are promising candidate materials with eco-friendly characteristics for industrial packaging applications. PHBV is a polyester obtained mainly by microbial production and stands out for being able to decompose in different environments, under aerobic and anaerobic conditions.[14,15] Moreover, PHBV is a semicrystalline polymer (~60% crystallinity degree), with a good barrier to water vapor and oxygen.[10] In addition, PHBV has mechanical properties similar to polypropylene, *e.g.*, Young's modulus (1.7 GPa) and tensile strength (38 MPa).[16]

However, PHBV is considered brittle and thermally unstable under processing conditions.[9,10] One of the widely used strategies to improve the processing and application of these polymers is the fabrication of nanocomposites, where the incorporation of nanoparticles might modulate their mechanical and barrier properties.[1] Sepiolite clay mineral (Sep) has a fibrous needle-shaped porous morphology composed of two tetrahedral silica sheets sandwiching a central octahedral magnesium hydroxide-oxide sheet that belongs to the 2 : 1 phyllosilicate mineral group.[17] It presents a high specific surface area and silanol groups (Si–OH) in the external surface, which can be used for organic modification or interaction with polymer matrices and other compounds through hydrogen bonds, dipole–dipole interactions, and van der Waals intermolecular interactions.[17–19] In our previous studies, Costa *et al.*[13] showed that the uniformly dispersed Sep nanoparticles in the PHBV matrix promoted a nucleating effect, which increased the degree of crystallinity from 66% for pure PHBV to 80% for PHBV/Sep, improved thermal stability, and promoted a higher barrier property reducing oxygen permeability by more than 70%. Similarly, Masood, Haider and Yasin[20] found that the good dispersion of Sep in the poly(3-hydroxyoctanoate) (PHO) matrix promoted significant improvements in elongation at break and tensile strength compared to the pure film.

Another approach to improving PHBV properties is the external plasticization, a simple and efficient approach where low molar mass compounds are directly mixed with the polymer matrix. The interaction between the polymer chains and the plasticizer increases the free volume and thus the mobility of the macromolecules, thus improving processing characteristics and mechanical behavior.[21,22] The incorporation of EOs might promote this plasticizing effect, thus altering the physical–mechanical properties and biodegradation behavior of the polymer.[13,15,23]

When combined with nanoparticles, the diffusion of the essential oil through the polymer matrix might be altered, resulting in distinct release kinetics depending on the composition and the medium, also affecting the antimicrobial activity.[24] Cândido *et al.*[25] observed that clove essential oil in cellulose acetate/montmorillonite nanocomposites provided bacteriostatic and antioxidant action during the storage of ham, which may be related to eugenol as the active compound present in the essential oil. The antimicrobial activity of oregano essential oil and the extension of the shelf life of fish for a further 10 days under refrigeration were also highlighted in the study of Cardoso *et al.*[26] with poly(butylene adipate *co*-terephthalate) (PBAT) film.

In this work, poly(hydroxybutyrate-*co*-hydroxyvalerate)/sepiolite nanocomposites were prepared using three different essential oils (EOs) (oregano – OEO, rosemary – REO, and basil – BEO). The chemical, physical and microbiological effects of each oil on the properties of the films were evaluated, in order to establish a relationship between the oil characteristics, the release kinetics, and antimicrobial activity of the films for application in antibacterial food packaging. Finally, the *in situ* antimicrobial activity of the films was analyzed by direct contact with mozzarella cheese against two bacteria: *Listeria monocytogenes* and *Escherichia coli* under simulated storage conditions at 5 °C.

2 Materials and methods

2.1 Materials

PHBV was supplied by Ningbo Tianan Biologic Material Co., Ltd (ENMAT Y 1000) with a viscosimetric molecular weight of 450

000 g mol^{-1} and a valerate content of 3.4 mol% (estimated by ^1H NMR solution ($CDCl_3$) spectroscopy). Oregano, rosemary, and basil essential oils, and sepiolite (Sep) were obtained from Sigma-Aldrich.

2.2 Film production

PHBV nanocomposites were prepared by melt processing using a Roller-Rotors R600, Rheomix 6002C mixer. PHBV and Sep were previously dried in an air circulation oven at 80 °C for 4 h. The processing was performed at 170 °C (for the pure PHBV film) and 165 °C (for the compositions with essential oils) at 100 rpm for 6 min. The materials were milled in a knife mill (SL-32 Solab Equipamentos) and compression molded at 190 °C and 1 ton for 2 min in a heated hydraulic press (SL-11 Solab Equipamentos).

2.3 Characterization of the essential oils

The composition and chemical structures of EOs were evaluated by gas chromatography-mass spectrometry (GC-MS) on an Agilent GC 7890A instrument coupled with an MS detector Agilent 5975C. The column, an HP-5MS (Agilent) fused silica capillary column (30 m length × 250 μm i.d. × 0.25 μm film thickness composed of 5% phenyl-95% methylpolysiloxane), was connected to an EI source (electron impact ionization) operating at 70 eV with a quadrupole mass analyzer. The mass scan ranged from 41 to 415 *m*/*z*. Helium was used as the carrier gas at a flow rate of 1.0 mL min^{-1}. The injector (with a split ratio of 1 : 20) and interface temperatures were 220 °C and 240 °C, respectively. The solvent delay was 3.0 min. The injection volume was 0.1 μL (10% v/v) with an autosampler Agilent GC Sampler 80 equipped with a 10 μL syringe. The oven temperature program consisted of ramping up from 60 °C (3 °C min^{-1}) to 246 °C, total run time of 62 min. The compounds were identified by comparing their mass spectra with those from the National Institute of Standards and Technology (NIST, 2011).[27] The Attenuated Total Reflectance – Fourier Transform Infrared Spectroscopy (ATR-FTIR) analysis was performed in a PerkinElmer Frontier equipment, with a resolution of 4 cm^{-1} and 16 scans from 4000 cm^{-1} to 450 cm^{-1}. Thermal characteristics of the essential oils were analyzed by thermogravimetric analysis (TGA) in PerkinElmer TGA 8000 equipment from 30 °C to 700 °C with a heating rate of 20 °C min^{-1} under an argon atmosphere (20 mL min^{-1}).

2.4 Characterization of the nanocomposites

2.4.1 Chemical characteristics and morphology. The chemical characteristics of the PHBV nanocomposites were investigated by ATR-FTIR analysis using the same parameters previously described. The spectra were normalized on a reference band at 1453 cm^{-1} assigned to the C–H asymmetric bending, which is known as a suitable internal standard.[28]

The morphology of the samples was evaluated by scanning electron microscopy (SEM) using JEOL JSM – 6390LV equipment using an acceleration of 15 kV. The samples were fractured by immersion in liquid N_2 in order to investigate the microstructure of the cross-section, and, after being fractured, samples were covered by a thin a layer of gold.

The hydrophobicity of the PHBV nanocomposites was studied using water contact angle measurements using a ramé-Hart 250 goniometer with Drop Image software. The measurements were obtained after direct deposition of distilled water droplets (3 μL) on the film surface of each sample sizing 1.0 cm × 3.0 cm. The experiments were performed in triplicate, and the average and standard deviation were calculated.

2.4.2 Thermal and dynamic-mechanical characteristics. Thermal characteristics were analyzed by thermogravimetric analysis (TGA) and differential scanning calorimetry (DSC). TGA analyses were performed using the same parameters previously described. DSC analysis was performed on TA Instruments Q20 equipment. The samples were analyzed from 40 °C to 200 °C at a heating and cooling rate of 10 °C min^{-1} under a nitrogen atmosphere (50 mL min^{-1}). The degree of crystallinity was determined using $\Delta H°m = 146$ J g^{-1} for PHBV.[29] The dynamic-mechanical thermal analysis (DMA) was performed in a TA Instruments Discovery DMA 850 in the tension film mode at 1 Hz, 4 N applied force and amplitude of 10 μm in the temperature range of −30 °C to 120 °C and a heating rate of 3 °C min^{-1}.

2.4.3 Controlled release of essential oils. To determine the release rate of essential oils from the films, 3% (v/v) acetic acid solution was used as a simulant for foods with a pH lower than 4.5, such as fermented milk, cream, juices containing fruit pulp, and cheeses preserved in water (fresh cheeses and mozzarella).[30] The samples (150 mg) were immersed in 30 mL of simulant and the system was continuously stirred at 100 rpm and 25 °C for 72 h in a MK1210 – TR orbital shaker. Aliquots of 2 mL were withdrawn periodically and replaced by an equal volume of simulant, and the concentration data were corrected. The EOs release (%) was determined by absorbance measurements using a Shimadzu UV-Vis 1800 spectrophotometer. The experiments were performed in triplicate, and the average value and standard deviation were reported.

2.4.4 Antibacterial activity and *in situ* antimicrobial activity evaluated in mozzarella cheese. The antibacterial activity of the films was evaluated according to JIS Z 2801:2000, with modifications, against Gram-negative *Escherichia coli* (*E. coli* ATCC 25922) and Gram-positive *Staphylococcus aureus* (*S. aureus* ATCC 25923) bacteria. All samples were previously exposed to UV-C light (200 nm to 280 nm) for 15 min for sterilization. Then, 0.4 mL of microbial inoculum (1.6×10^4 CFU mL^{-1}) was placed on the surface of the films (5 cm × 5 cm) and covered with the inert film (4 cm × 4 cm), ensuring close contact with the antibacterial surface. The samples were incubated at 35 °C and 90% relative humidity for 24 h. After incubation, the films were carefully washed with 10 mL of 0.1% peptone solution with 0.7% Tween 80. For viable cell count, 1 mL was transferred to a tube containing 9 mL of 0.1% peptone and serially diluted. The tests were performed in triplicate and the average and standard deviation were calculated. The antibacterial activity was calculated according to eqn (1), where *R* is the value of antibacterial activity (log CFU mL^{-1}), *A* is the mean of bacterial counts in the control sample after 24 h (inoculum), and *B* is the mean of bacterial counts of the test sample after 24 h.

$$R = \log(A/B) \quad (1)$$

In order to ensure the effectiveness of the films in a real application throughout a food supply chain (*i.e.*, cold chain and ambient storage),[31] an *in situ* antibacterial activity test was carried out based on the storage conditions of the target product (mozzarella cheese, kept at 5 °C). The *in situ* antimicrobial activity test was conducted using suspensions of *E. coli* ATCC 25922 at 10^5 CFU mL^{-1} and of *Listeria monocytogenes* ATCC 13627 at 10^6 CFU mL^{-1}. The bacteria were reactivated separately in Brain Heart Infusion (BHI) broth, incubated at 35 °C (±1 °C) for 18 h and the suspension adjusted to the McFarland 0.5 standard containing approximately 1.5×10^5 CFU mL^{-1}. Mozzarella cheese slices (obtained commercially from a local market from Florianópolis – Brazil), their respective interleaves (inert film used as control) and the formulation of interest (PHBV/sepiolite/oregano essential oil film, hereafter abbreviated as POSep film) were cut into 4 cm × 4 cm squares. Subsequently, the POSep film was sterilized under UV light for 15 min on each side. Then, 100 μL of each bacterial suspension was placed in direct contact with the surface of the cheeses and covered with the POSep film. Combinations of cheese and inert film were also prepared as a control. The samples were packaged in sealed plastic bags and kept at 5 °C ± 1 °C in order to simulate storage conditions. The microbiological count in the cheese was evaluated after 3, 6, 9, 12, 15, and 30 days. All the analyses were carried out in triplicate and the average and standard deviation were determined.

For the microbiological analysis, the mozzarella cheese was separated from the film and placed in a sterile plastic bag (Stomacher – Laborclin) and homogenized with 0.1% peptone (1 : 10) for about 1 min at 250 rpm using a Bag Mixer (Interscience).[32] Then, 1 mL of the resulting broth was collected, diluted and inoculated into a Petri dish with Tryptone Bile X-glucuronide Agar (TBX) for counting *E. coli*. For the *L. monocytogenes*, 100 μL of the broth was inoculated into an Agar Listeria according to Ottaviani and Agosti Agar medium (ALOA). All the Petri dishes were incubated at 37 °C, and the microbiological counts were determined after 24 h and 48 h, respectively.

3 Results and discussion

3.1 Characterization of the essential oils

The selection of the three different commercial oils used in this work was due to their distinct compounds, aiming to obtain the best oil/clay/polymer combination to optimize the physical–chemical and antimicrobial properties of the proposed active packaging. Initially, the constituents of the three commercial oils were identified using GC-MS analyses (ESI Fig. 1†). For OEO, the chromatogram indicated that 3-methyl-4-isopropylphenol was the major compound (71.7%), followed by benzene (14.9%) and γ-terpinene (6.9%). The major compound found in the REO was eucalyptol (or 1,8-cineole) with 60.8% of the composition, followed by 14.7% of α-pinene. For BEO, the basic compound identified was estragole (99.3%). The compositions of the essential oils are in good agreement with those reported in the literature.[33] The differences found for OEO, in which carvacrol or thymol are the major compounds found in the literature,[34–36] are justified by the dependence of EOs composition on the region of extraction of the oil, the specific part of the plant from which the oil is extracted (*e.g.* leaves, fruit, or stems), and, finally, the method used to extract the oil.[35]

ATR-FTIR analysis confirmed the main chemical structures present in each oil (Fig. 1a). The OEO spectrum shows a broad peak at 3450 cm^{-1}, attributed to the hydroxyl of the phenolic compounds. In addition, the band at 1200 cm^{-1} refers to the C–O group of phenols. The sharp characteristic bands at 2983 cm^{-1} are related to the C–H stretching, at 1458 cm^{-1} to the CH_2 bending, at 1253 cm^{-1} to the C–O–C stretching, and at 937 cm^{-1} to the C–H bending.[37,38] The REO spectrum shows intense bands at 985 cm^{-1}, attributed to the C–O bond of the eucalyptus ether.[39] Besides, the bands at 2922 cm^{-1} and 2945 cm^{-1} are characteristics of the symmetric and asymmetric stretching vibration of the C–H and CH_2, respectively.[40] Finally, the BEO spectrum shows two intense bands at 1510 and 1241 cm^{-1}, attributed to the C=C vibration of aromatics, at 2835 cm^{-1} attributed to the C–H stretching, and at 1100 cm^{-1} characteristic of the C–O–C ether bond.[41]

Fig. 1b shows the TGA and DTG curves of the oils. OEO exhibited two thermal events related to its various compounds. The first loss of mass between 80 °C and 198 °C corresponds to the volatilization of lower boiling point compounds such as benzene (80 °C) and γ-terpinene (167 °C to 178 °C), and the second loss of mass between 198 °C and 270 °C might be related to the complete volatilization of compounds such as 3-methyl-4-isopropylphenol, which is in accordance with the boiling point of the oil at 246 °C.[37,42] Two thermal events in the TGA curve were also observed for REO, with the first mass loss around 100 °C, related to eucalyptol, whose boiling point is 176 °C,[43] and a less pronounced second mass loss at 350 °C, attributed to other minor components present in this oil. These characteristic degradation profiles corroborate the multiple composition of the oils, as shown by the GC-MS analyses. In contrast, BEO showed a single loss of mass in the temperature range between 60 °C and 210 °C corresponding to the complete volatilization of REO. This behavior can also be related to its composition (99.3% estragole, with a boiling point around 216 °C).[44]

3.2 Nanocomposites characterization

3.2.1 Chemical analyses and morphology. The ATR-FTIR spectra of the pure PHBV (hereafter abbreviated as P), PHBV/essential oil compositions (PHBV/OEO, PHBV/REO, and PHBV/BEO, hereafter abbreviated as PO, PR, and PB, respectively), PHBV/sepiolite (PSep) and PHBV/oil/clay compositions (PHBV/OEO/sepiolite, PHBV/REO/sepiolite, and PHBV/BEO/sepiolite, hereafter abbreviated as POSep, PRSep, and PBSep, respectively) are shown in Fig. 2. The comparison between the spectra identifies the dominant bands associated with PHBV. The band at 3440 cm^{-1} is assigned to adsorbed moisture. The bands at 2977 cm^{-1} and 2934 cm^{-1} represent the asymmetric and symmetric stretching vibrations of the C–H bond, respectively, while the high intensity band at 1710 cm^{-1} is related to the stretching of the ester carbonyl (C=O).[45] An increase in the intensity of the band at 3440 cm^{-1} can be noted for the films

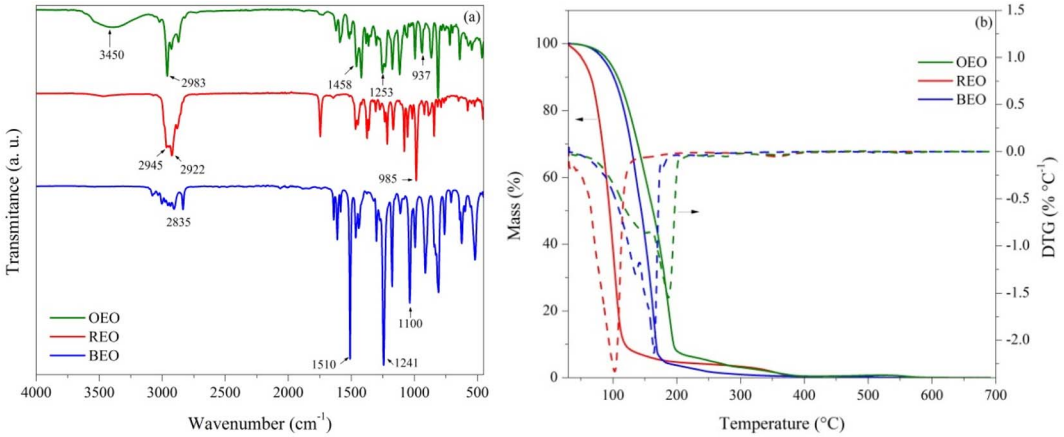

Fig. 1 (a) ATR-FTIR spectra and (b) TGA and DTG curves of the OEO, REO and BEO (solid lines: TGA curves; dashed lines: DTG curves).

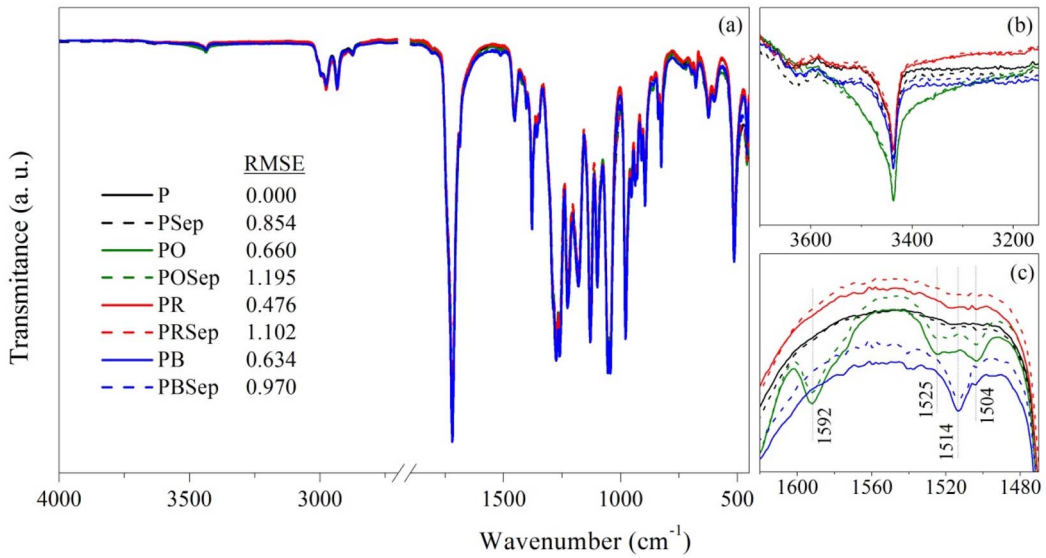

Fig. 2 (a) ATR-FTIR spectra of pure PHBV and PHBV compositions containing sepiolite (dashed lines) and different essential oils; (b) and (c) details of the main changes observed.

containing OEO (Fig. 2b), and might be related to the broad band at 3450 cm^{-1} of OEO attributed to the hydroxyl of phenolic compounds found in its composition. Additionally, some new bands in the range of 1600 cm^{-1} to 1500 cm^{-1}, related to aromatic systems, are visible for the films containing OEO and BEO (Fig. 2c).

Since the difference between the compositions is not clearly visible, a comparison between the spectra was followed by adjustment using the method of least squares (RMSE).[13] The RMSE value for pure PHBV is 0.000 since the comparison is made with the spectrum itself. An increase in the RMSE of PSep films confirms that the nanoparticle was incorporated into the films and that the polymer–filler interaction is more pronounced than with the EOs, since lower RMSE values were found for PO, PR and PB films. This higher interaction might be related to the presence of silanol groups on the external surface of Sep which might interact with carbonyl groups of PHBV through intermolecular interactions. The combination between the two additives (oil and clay) results in a greater linearity deviation between the spectra, increasing the RMSE values to close to 1. The higher value of RMSE for POSep films might indicate the favored incorporation of OEO in the materials produced. Considering the major compounds found in the composition of EOs (GC-MS analyses), distinct interactions with Sep and PHBV might be expected, being stronger for OEO due to the hydroxyl groups from its phenolic compounds.

SEM micrographs were performed to evaluate the interface and dispersion of components in the PHBV matrix and the characteristics of the films according to each type of essential oil (Fig. 3). PHBV films containing essential oils exhibited a slightly higher roughness when compared to pure PHBV. The plasticizing effect of the oils increases the mobility of polymer chains, consequently improving the ductility of the polymer matrix. With the Sep incorporation, it is possible to observe

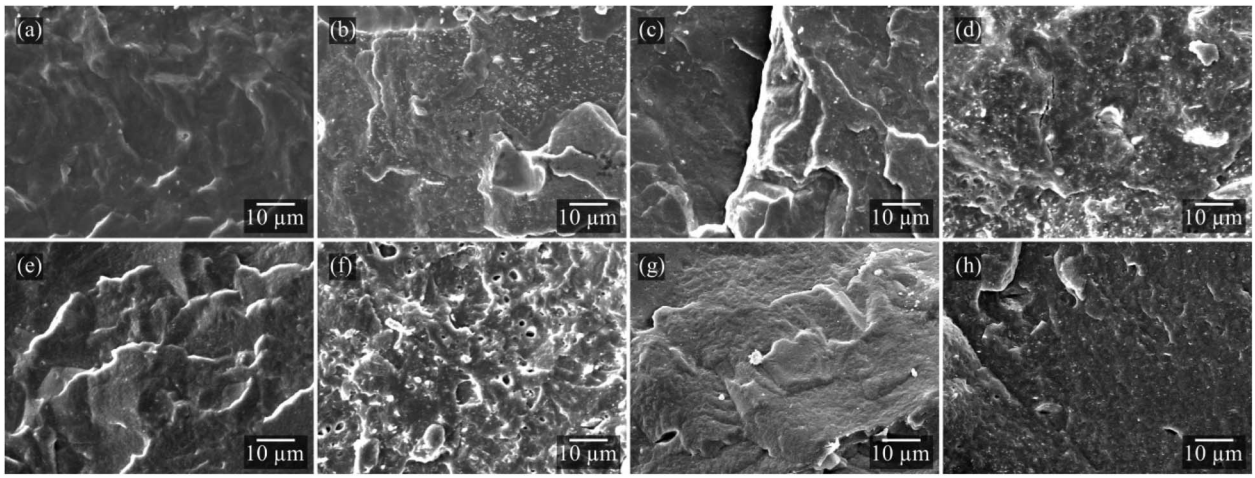

Fig. 3 SEM micrographs of (a) P, (b) PSep, (c) PO, (d) POSep, (e) PR, (f) PRSep, (g) PB, and (h) PBSep compositions.

some fine dispersed nanoparticles, especially for POSep and PBSep compositions (Fig. 3d and h). The homogeneous dispersion of Sep nanoparticles (light color particles in SEM images) indicates a stronger interaction of the clay mineral and PHBV matrix in the presence of OEO and BEO, respectively. In contrast, the PRSep films (Fig. 3f) presented a porous and heterogeneous appearance, which might be indicative of a low compatibility between the additives and the polymeric matrix.[21] The observed voids might refer to the loss of REO due to its volatilization during the analysis.

The incorporation of clay minerals modifies both surface and bulk properties of the polymer, including surface roughness and wettability, and thermal and mechanical properties.[46] The characteristics of the films' surface affect its water resistance and influence the release of active compounds from oils during product storage and use.

All samples presented similar wettability (Fig. 4). For the pure PHBV film (P), a contact angle of 82.28° ± 3.17° was found, which is in accordance with the literature.[46,47] The contact angle values slightly increased with the addition of essential oils. The reduction in the hydrophilic character with the incorporation of oils provides higher water resistance to the films, which is desirable for biodegradable films to protect the food throughout its shelf life.[48] It is also possible to highlight a tendency towards an increase in the contact angle with the incorporation of Sep in PHBV films, mainly in the PSep and POSep combination. This increase may be indicative of the interaction between the nanoparticles and the OEO, reducing the interaction of the free hydrophilic groups with water and, consequently, increasing the contact angle.[48] Besides hydrophobicity, the contact angle of the polymer also depends on the roughness of the surface,[46,49,50] as observed by Farmahini-Farahani *et al.*[46] for PHBV/montmorillonite Cloisite 30B, Lemes *et al.*[49] for PHBV/multi-walled carbon nanotubes (MWCNTs), and Conceição *et al.*[50] for PHBV/short cellulose fibers. The incorporation of sepiolite might impart an increased roughness for the nanocomposites, thus increasing the contact angle.

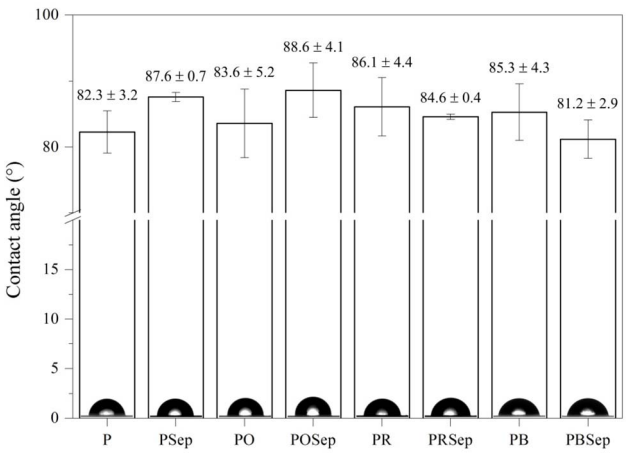

Fig. 4 Contact angle measurements of pure PHBV and PHBV compositions.

3.2.2 Thermal and dynamic-mechanical characteristics. All compositions containing antimicrobial additives exhibit a mass loss regarding the volatilization of oil compounds up to 270 °C. Therefore, the real oil content in each composition was determined from the residual mass at 255 °C, and varied from 2.2% to 3.3%.

It is well known that PHBV degradation occurs in one mass loss step in the range of 265 °C to 319 °C, with a maximum degradation rate temperature ($T_{d_{PHBV}}$) of 308 °C (ESI material Fig. 2† and Table 1), following a random chain scission mechanism (*cis* elimination).[45,51] PB and PBSep compositions presented high thermal stability compared to the pure PHBV film, related to the higher boiling point of BEO compared to the other oils used, as already discussed in TGA analysis.

It is possible to visualize an increase in the thermal degradation temperature of the films in the presence of the nanoparticles. This increase might be attributed to the dispersion of the filler in the polymer matrix, creating a barrier effect to heat and volatile degradation products,[19] and to the polymer–filler interaction to strengthen the material's structure.[11] The clay

Table 1 TGA, DSC, and DMA results for PHBV compositions

	TGA				DSC			DMA	
Sample	$T_{d_{EO}}$ (°C)	$T_{d_{PHBV}}$ (°C)	EO (%)	Sep (%)	T_c (°C)	T_m (°C)	X_c (%)	E' 25 °C (GPa)	T_g (°C)
P	—	308	—	—	84	169/176	63	3.28	18.8
PSep	—	309	—	2.4	91	170/174	63	3.33	13.5
PO	159	296	3.3	—	82	166/174	64	1.94	15.6
POSep	166	308	3.2	2.4	88	168/174	66	2.22	10.8
PR	161	308	3.0	—	83	169/175	67	3.28	14.9
PRSep	160	310	2.8	2.7	87	168/174	68	3.23	18.3
PB	168	311	2.2	—	89	169/175	68	4.03	8.7
PBSep	178	309	2.3	2.0	92	170/174	69	3.08	12.5

content was calculated from the residue at 690 °C. The incorporated clay content varied between 2.0% and 2.7% in the compositions. This variation in the mass of incorporated nanoparticles between the different formulations did not directly influence the thermal stability of the films, since all temperatures of maximum degradation rate ($T_{d_{PHBV}}$) of the nanocomposites were similar.

The crystallization temperature (T_c) obtained for the pure PHBV film (ESI Fig. 3a†) resembles that obtained for the PR and PO films. The incorporation of nanoparticles into a polymer matrix might provide additional sites for the formation of crystalline nuclei.[11,12] For the PHBV compositions containing Sep, the increase in T_c confirms the nucleating effect of nanoparticles on PHBV crystallization. Similar results were found by Yan *et al.*[12] in PBAT compositions containing cellulose nanocrystals (CNCs), in which CNC acted as a heterogeneous nucleating agent.

A double melting peak profile (ESI Fig. 3b†) was observed in all formulations. The second melting peak (T_{m2}) was more pronounced in P, PO, and PR films than the T_{m1} peak. With the addition of nanoparticles, however, the peaks corresponding to T_{m1} showed greater intensity, especially in the POSep and PBSep compositions, indicating different spherulitic structures in the films and confirming the nucleating effect of Sep. An increase in the crystallinity of all compositions is also worth noting, especially for formulations containing BEO. The agglomeration of Sep nanoparticles in PBSep films might be responsible for the formation of crystalline nuclei, consequently increasing the crystallinity of the films.

The glass transition temperature (T_g) of the pure PHBV was 18.8 °C (Fig. 5a). In general, the T_g values were reduced, indicating a higher mobility of the amorphous phase, making the material more flexible at room temperature and improving the mechanical performance of these formulations as flexible films for application in foods. The PB composition showed the lower T_g value (8.7 °C). The similarity between the solubility parameter of BEO and PHBV corroborates the strong interaction between these compounds, resulting in a higher plasticizing effect in the polymer matrix. However, the mechanical performance decreased with the presence of Sep in PBSep compositions when compared to the PB sample, with the value of E' reduced to 3.08 GPa at 25 °C (Fig. 5b). This is additional evidence for the low interaction of Sep with BEO that resulted in poor dispersion of the nanoparticles, as observed by SEM micrographs.

The films containing REO (PR and PRSep) did not exhibit significant differences in T_g and storage modulus (E'), indicating a limited interaction between the components. Conversely, PO films showed lower stiffness at room temperature which increased with the incorporation of Sep. This effect indicates that the incorporation of OEO into the PHBV matrix together with nanoparticles can contribute to an increase in interactions between the components, thus resulting in a tougher material. As a result, the performance of the films for packaging applications can be adjusted with the appropriate selection of the clay/oil system, producing materials with functional properties.

The addition of EOs increased the dissipation of energy in the materials, resulting in higher E'' and tan δ values in all the temperature ranges. The increased mobility promoted by the EOs increased the energy damping capacity of the polymer,[52] in which the material loses energy to molecular rearrangements and internal friction.[53] The restriction on the mobility of the polymer chains promoted an opposite effect, especially in POSep composition where the particle/polymer interactions were higher and increased the elastic response of the material.

3.2.3 Controlled release. For application in active packaging, a controlled release of the active compound through the polymer matrix is required in order to maintain a minimum inhibitory concentration to avoid spoilage.[54] However, the release kinetics depends on the properties and composition of the polymer and of the active compounds[34] and also depends on the type of food in which the material will come into contact, since each food has specific polarity, acidity, and humidity conditions.[24] For example, for high fat content foods, the migration of EOs tends to be faster and higher due to the lipophilic nature of their low molecular weight compounds. Aiming at our target application, a 3% v/v acetic acid solution was used to simulate low pH aqueous foods, such as fermented milk, cream, juices containing fruit pulp, and cheeses preserved in water (fresh cheeses and mozzarella), following the Commission Regulation (EU) no. 10/2011 (2011).[30]

The release profile of different EOs exhibited variations according to the oil composition, while the presence of Sep, in

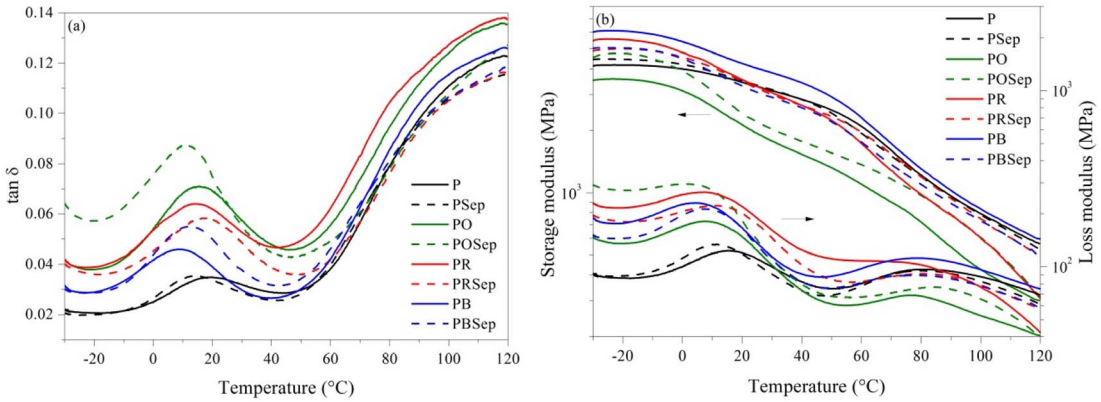

Fig. 5 (a) Tan δ and (b) storage (E') and loss (E'') modulus results for pure PHBV and PHBV compositions (solid lines: compositions without sepiolite; dashed lines: compositions with sepiolite).

general, did not influence this process (Fig. 6). The release of OEO occurred gradually, irrespective of the presence of Sep. In contrast, the release of BEO in the medium was detected only after 24 h, reaching a maximum of ~7.4% in 48 h. The films containing REO exhibited a lower initial rate, but a higher release rate after 24 h, reaching up to 39.8% ± 1.4% after 48 h for PRSep films.

The partition coefficient ($K_{P/L(a)}$, Table 2) is a parameter that can be used to evaluate the distribution of the essential oil in the polymer or in the medium, thus providing information about the affinity between the components. It is defined as the ratio of the difference between the solubility parameter of the medium (L) and the solubility parameter of the oil (a) ($\Delta\delta_{L,a}$), and the difference between the solubility parameters of the polymer (P) and the oil (a) ($\Delta\delta_{P,a}$) (eqn (2)).[56]

$$K_{P/L(a)} = \frac{\Delta\delta_{L,a}}{\Delta\delta_{P,a}} \quad (2)$$

The lower $K_{P/L(a)}$ value found for OEO indicates a greater partition coefficient with the medium and, consequently, the higher diffusion of the active compound through the polymer matrix. Therefore, even though a greater interaction of OEO was observed in compositions with PHBV, its greater affinity with the medium is the preponderant factor that results in a faster release in the first 24 h. For BEO, the higher $K_{P/L(a)}$ value indicates a slow migration of the oil to the medium. In addition to the high $K_{P/L(a)}$, it is possible to observe similar values of δ between BEO and PHBV, evidencing the greater interaction between the phases.

The $K_{P/L(a)}$ value of REO was intermediate to that obtained for OEO and BEO, and is coherent with the release results obtained up to 6 h. For longer times, other factors might have influenced the high release rate observed, such as the liquid diffusion into the polymer chains and the diffusion of the active compound from the polymer matrix to the medium.[24,35] The poor dispersion of Sep in these films might have favored the diffusion of the oil throughout the film.

3.2.4 Antibacterial activity and *in situ* antimicrobial activity evaluated in mozzarella cheese. The chemical structure of the individual EOs components affects both mode of action and antibacterial activity. The mode of action of EOs in bacterial cells includes degradation of the cell wall, damages to the cytoplasmic membrane and to membrane proteins, leakage of cell contents, disruption of the proton motive force, and coagulation of cell contents.[6] The wide range of active compounds found in EOs obtained from aromatic plants – especially those with a high percentage of phenolic compounds – are

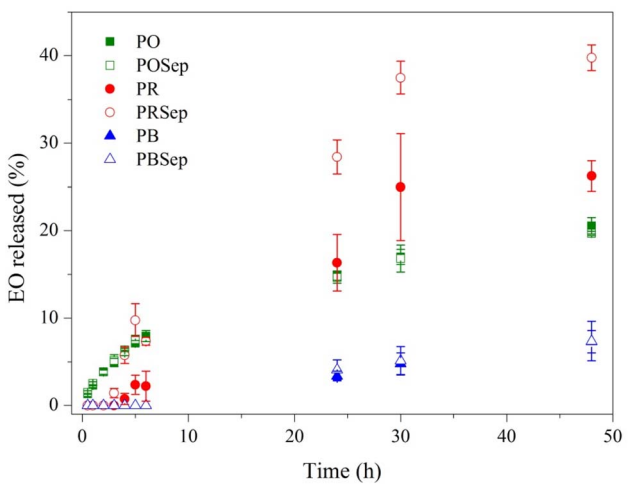

Fig. 6 Release of essential oils from PHBV compositions.

Table 2 Solubility parameter (δ) and partition coefficient ($K_{P/L(a)}$) of PHBV, acetic acid, and major compounds of each EO

Substance	Solubility parameter (δ) ($MPa^{1/2}$)	Partition coefficient ($K_{P/L(a)}$)
PHBV	20.6 (ref. 55)	—
Acetic acid 3% v/v	47.1 (ref. 56)	—
OEO	15.1 (ref. 57)	5.82
REO	17.8 (ref. 58)	10.46
BEO	19.2 (ref. 58)	19.93

Table 3 Antibacterial activity of PHBV compositions against *E. coli* and *S. aureus*

	E. coli		*S. aureus*	
Sample	Reduction (log)	Reduction (%)	Reduction (log)	Reduction (%)
PO	3.0 ± 0.5	99.9	4.4 ± 0.9	99.9
POSep	2.4 ± 0.8	99.6	3.2 ± 0.9	99.9
PR	0.0 ± 0.0	6.3	0.3 ± 0.3	54.3
PRSep	0.2 ± 0.5	31.3	0.6 ± 0.0	75.7
PB	3.2 ± 0.8	99.9	6.0 ± 0.0	99.9
PBSep	0.2 ± 0.1	39.2	0.3 ± 0.3	54.3

responsible for the antimicrobial activity aimed for application in active food packaging.[47]

The counts of *S. aureus* in PO and POSep films confirmed the antimicrobial characteristic of the films, with a log reduction of 4.4 for the PO and 3.2 for the POSep film (Table 3). The composition PB also showed great performance against Gram-positive bacteria, with a log reduction of 6.0, indicating a 99.9% reduction in microbial growth. Although lower, the presence of BEO in films of PHBV was effective against *E. coli*, reaching a value of 3.2 log. However, the addition of Sep resulted in a reduced antimicrobial activity of PBSep composition. The presence of poorly dispersed BEO and sepiolite in these films might have harmed the properties of the material, consequently reducing the contact of the BEO with the inoculum.

Similar behavior was found in PRSep films, with significantly low reduction values. Additionally, PR films exhibited lower antibacterial activity against both bacteria. In these cases, the slow-release profile in the first 24 h might result in an insufficient concentration of the antimicrobial agent to prevent microbial growth. The quick release of the active compound after that might not sustain the minimum inhibitory concentration for long periods.

These results evidence that, in general, there are differences regarding the effectiveness of the different essential oils on the antibacterial activity. These differences might be related to the variation in the penetration rate of the extracts into the cell wall and the structures of the cell membranes, and also to the susceptibility of the microorganisms. Among the three EOs tested, OEO was the most effective, reaching reduction values higher than 99.9% for both bacteria. These results corroborate the finds obtained in the release test, in which OEO exhibited a faster release in the first 24 h, contributing to the inhibition of bacterial growth at the early stages of spoilage. This oil is considered as one of the most useful antimicrobial agents, and this property can be attributed to the high amount of phenolic compounds that constitute OEO, as well as to the synergistic effect with other minor components such as monoterpenes, hydrocarbons, γ-terpinene, and *p*-cymene.[6,48]

Concerning the bacteria type, most studies agree that EOs are generally more active against Gram-positive than Gram-negative bacteria,[6] once the latter possesses an outer membrane surrounding the cell wall that restricts diffusion of hydrophobic compounds. In this study, all EOs evaluated exhibited a better performance against Gram-positive bacteria. Similar results were found by Hashemi *et al.*[48] using OEO in basil seed gum edible films, by Amor *et al.*[59] using BEO in chitosan films, and by Garcia-Sotelo *et al.*[60] using REO encapsulated within β-cyclodextrin (β-CD).

Thus, this set of results indicates that POSep composition is responsible for the best performance as active packaging. Therefore, this composition was selected to evaluate the *in situ* activity, simulating refrigerated storage conditions of mozzarella cheese (5 °C).

An *in situ* antimicrobial test was carried out using two of the most common pathogenic bacteria found in mozzarella cheese, *i.e.*, *L. monocytogenes* (Gram-positive) and *E. coli* (Gram-negative) (Fig. 7). *L. monocytogenes* was included in the cheese tests because it is an important foodborne pathogen. Cheese has historically been involved in outbreaks caused by *L. monocytogenes* around the world and this bacterium represents a major challenge for the food industry.

For both bacteria, the greatest reduction of inoculum on the mozzarella cheese occurred in the initial contact time, highlighting the reduction of 10^1 CFU mL^{-1} after three days for *E. coli* and after six days for *L. monocytogenes* on POSep films. Compared to the control sample, there was a higher inhibition in active films, potentially attributable to a greater initial release of the active compound, as evidenced by the OEO release test in food simulated medium. After this period, there was a fluctuation in the microbial counts between 10^3 and 10^4 CFU mL^{-1}, without a significant inhibition. Han *et al.* (2014)[61] also found that antimicrobial sachets containing rosemary and thyme essential oils were not able to completely eliminate *L. monocytogenes* in contact with cheese. However, the presence of the sachets resulted in a slower growth and a lower count of bacteria until 12 days.

Dannenberg *et al.*[62] found similar effects of cellulose acetate films containing pink pepper essential oil against *L. monocytogenes* in *in situ* analysis using mozzarella cheese. After three days, the microbial counts were significantly lower than the control sample, indicating the greatest release of the oil during this period, justified by the affinity between the non-polar components of the oil and the cheese, which is composed of approximately 21% of lipids.[62]

The low antimicrobial activity found in this work can be associated with the refrigeration temperatures (5 °C ± 1 °C), where the diffusion of the OEO might be lower than that proposed in dissolution tests (simulated at 25 °C). Hence, the higher inhibition observed in the early stages might be related to the oil present near the surface of the films, readily available for contact with the food. It is worth highlighting that *L. monocytogenes* is a psychrotrophic bacterium that has the ability to grow over a wide temperature range, varying from 0.4 to 45 °C, and is highly pH- and salt-tolerant.[61,63] Even under these conditions, POSep films were able to inhibit the growth of the bacteria and the microbial count was lower than the control during all the period analyzed. Therefore, it can be considered that the films meet the requirements for the desired

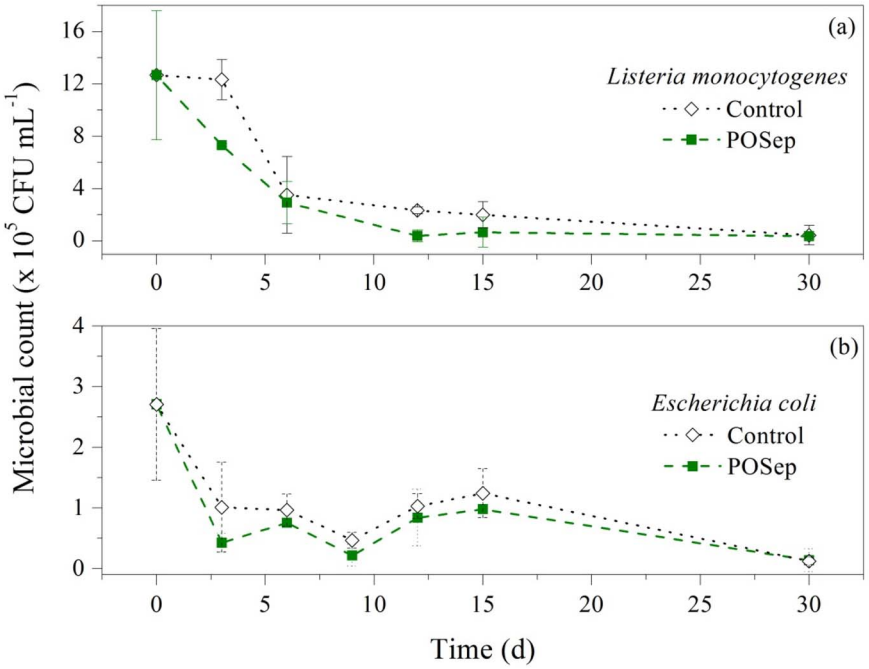

Fig. 7 *In situ* antimicrobial activity of POSep film by direct contact on mozzarella cheese for (a) *Listeria monocytogenes* and (b) *Escherichia coli*.

antimicrobial properties, exhibiting very promising results in the *in situ* tests.

4 Conclusion

The chemical composition of different essential oils directly influenced the interaction with the other components of the films. This effect was highlighted in the release tests, where the delivery of the antimicrobial additive strongly depends on the interaction of the oil with the polymer and this combination with the food simulating medium. BEO presented a solubility parameter close to that of PHBV, indicating affinity between the matrices, and the high partition coefficient made the release of the additive slower into the medium. This characteristic also affected the antibacterial activity, reducing their potential for microbial inhibition.

The POSep nanocomposite was the most promising for application in food packaging, with a faster OEO release in the first period and a controlled release in the remaining period, preventing the growth of the tested bacteria. The results indicated a satisfactory performance of the POSep films in relation to those used as controls, maintaining the microbiological count decreasing over the 30 days of testing. Therefore, the films containing PHBV, sepiolite and oregano essential oil proved to be suitable for application as packaging materials with antimicrobial properties and ensuring product safety.

Data availability

Data will be made available on request.

Conflicts of interest

There are no conflicts to declare.

Acknowledgements

The authors are grateful to Conselho Nacional de Desenvolvimento Científico e Tecnológico (CNPq – Process 313599/2018-1) and Coordenação de Aperfeiçoamento de Pessoal de Nível Superior/Fundação de Amparo à Pesquisa e Inovação do Estado de Santa Catarina (CAPES/FAPESC) for financial support. The authors also thank the Laboratório Central de Microscopia Eletrônica (LCME) from UFSC for the SEM analyses.

References

1 J. R. Westlake, M. W. Tran, Y. Jiang, X. Zhang, A. D. Burrows and M. Xie, *Sustainable Food Technol.*, 2023, **1**, 50–72.
2 J. R. Calo, P. G. Crandall, C. A. O'bryan and S. C. Ricke, *Food Control*, 2015, **54**, 111–119.
3 G. Biddeci, G. Cavallaro, F. D. Blasi, G. Lazzara, M. Massaro, S. Milioto, F. Parisi, S. Riela and G. Spinelli, *Carbohydr. Polym.*, 2016, **152**, 548–557.
4 A. M. Khaneghah, S. M. B. Hashemi and S. Limbo, *Food Bioprod. Process.*, 2018, **111**, 1–19.
5 N. Khorshidian, M. Yousefi, E. Khanniri and A. M. Mortazavian, *Innov. Food Sci. Emerg. Technol.*, 2018, **45**, 62–72.
6 S. Burt, *Int. J. Food Microbiol.*, 2004, **94**, 223–253.
7 K. Bazaka, M. V. Jacob, W. Chrzanowski and K. Ostrikov, *RSC Adv.*, 2015, **5**, 48739–48759.

8 C. Bonnenfant, N. Gontard and C. Aouf, *Polymer*, 2023, **270**, 125784.
9 X. Zhao, K. Cornish and Y. Vodovotz, *Environ. Sci. Technol.*, 2020, **54**, 4712–4732.
10 F. Jahangiri, A. K. Mohanty, A. K. Pal, S. Shankar, A. Rodriguez-Uribe, R. Clemmer, S. Gregori and M. Misra, *Prog. Org. Coat.*, 2024, **189**, 108270.
11 L. Yan, S. Y. H. Abdalkarim, X. Chen, Z. Chen, W. Lu, J. Zhu, M. Jin and H.-Y. Yu, *Compos. Sci. Technol.*, 2024, **245**, 110364.
12 L. Yan, G. Lu, S. Y. H. Abdalkarim, L. Wang, Z. Chen, W. Lu and H.-Y. Yu, *Int. J. Biol. Macromol.*, 2024, **255**, 128264.
13 R. C. D. Costa, T. S. Daitx, R. S. Mauler, N. M. D. Silva, M. Miotto, J. S. Crespo and L. N. Carli, *Food Packag. Shelf Life*, 2020, **26**, 100602.
14 M. Fernandes, A. Salvador, M. M. Alves and A. A. Vicente, *Polym. Degrad. Stab.*, 2020, **182**, 109408.
15 P. R. Oliveira, P. X. Mendoza, J. S. Crespo, T. S. Daitx and L. N. Carli, *Int. J. Biol. Macromol.*, 2024, **277**, 133768.
16 K. Sudesh, H. Abe and Y. Doi, *Prog. Polym. Sci.*, 2000, **25**, 1503–1555.
17 D. Nath, R. Santhosh, K. Pal and P. Sarkar, *Food Packag. Shelf Life*, 2022, **31**, 100803.
18 E. Ruiz-Hitzky, M. Darder, F. M. Fernandes, B. Wicklein, A. C. S. Anlcântara and P. Aranda, *Prog. Polym. Sci.*, 2013, **38**, 1392–1414.
19 J. González-Ausejo, J. Gámez-Pérez, R. Balart, J. M. Lagarón and L. Cabedo, *Polym. Compos.*, 2019, **40**, E156–E168.
20 F. Masood, H. Haider and T. Yasin, *Appl. Clay Sci.*, 2019, **175**, 130–138.
21 M. D. Slongo, S. D. F. Brandolt, T. S. Daitx, R. S. Mauler, M. Giovanela, J. S. Crespo and L. N. Carli, *J. Polym. Environ.*, 2018, **26**, 2290–2299.
22 S. D. F. Brandolt, T. S. Daitx, R. S. Mauler, H. L. Ornaghi Junior, J. S. Crespo and L. N. Carli, *Polym. Compos.*, 2019, **40**, 3835–3843.
23 P. R. Oliveira, R. C. D. Costa, D. S. Malvessi, T. S. Daitx, R. S. Mauler, M. Miotto, D. M. Bobermin, J. S. Crespo, C. S. Teixeira, I. C. Bellettini and L. N. Carli, *Appl. Clay Sci.*, 2023, **241**, 107004.
24 R. C. D. Costa, A. P. Ineichen, C. S. Teixeira, I. C. Bellettini and L. N. Carli, *Polímeros*, 2022, **32**, e2022028.
25 G. S. Cândido, M. S. Silva, N. J. Zaneratto, R. H. Piccoli, E. E. N. Carvalho and J. E. D. Oliveira, *ACS Appl. Nano Mater.*, 2024, DOI: **10.1021/acsanm.4c01235**.
26 L. G. Cardoso, J. C. P. Santos, G. P. Camilloto, A. L. Miranda, J. I. Druzian and A. G. Guimarães, *Ind. Crops Prod.*, 2017, **108**, 388–397.
27 R. P. Adams, *Identification of Essential Oil Components by Gas Chromatography/mass Spectrometry*, 2007.
28 J. D. Badia, T. Kittikorn, E. Strömberg, L. Santonja-Blasco, A. Martínez-Felipe, A. Riber-Greus, E. Ek and S. Karlsson, *Polym. Degrad. Stab.*, 2014, **108**, 166–174.
29 S. Gogolewski, M. Jovanovic, S. M. Perren, J. G. Dillon and M. K. Hughes, *Polym. Degrad. Stab.*, 1993, **40**, 313–322.
30 C. Regulation, *Commission Regulation (EU) No 10/2011 of 14 January 2011 on Plastic Materials and Articles Intended to Come into Contact with Food*, 2011.
31 Z. Miao, M. Yang, S. Y. H. Abdalkarim and H.-Y. Yu, *Int. J. Biol. Macromol.*, 2024, **279**, 135090.
32 M. Lotfi, H. Tajik, M. Moradi, M. Forough, E. Divsalar and B. Kuswandi, *LWT–Food Sci. Technol.*, 2018, **92**, 576–583.
33 D. Teneva, Z. Denkova, R. Denkova-Kostova, B. Goranov, G. Kostov, A. Slavchev, Y. Hristova-Ivanova, G. Uzunova and P. Degraeve, *Food Chem.*, 2021, **344**, 128707.
34 I. S. M. A. Tawakkal, M. J. Cran and S. W. Bigger, *LWT–Food Sci. Technol.*, 2016, **66**, 629–637.
35 I. Fernández-Pan, J. I. Maté, C. Gardrat and V. Coma, *Food Hydrocoll.*, 2015, **51**, 60–68.
36 R. Shemesh, M. Krepker, M. Natan, Y. Danin-Poleg, E. Banin, Y. Kashi, N. Nitzan, A. Vaxman and E. Segal, *RSC Adv.*, 2015, **5**, 87108.
37 S. F. Hosseini, M. Zandi, M. Rezaei and F. Farahmandghavi, *Carbohydr. Polym.*, 2013, **95**, 50–56.
38 A. A. Oun, A. Y. Bae, G. H. Shin, M.-K. Park and J. T. Kim, *Appl. Clay Sci.*, 2022, **224**, 106522.
39 S. Hamiche, N. Bouzidi, Y. Daghbouche, A. Badis, S. Garrigues, M. D. L. Guardia and M. El Hattab, *Sustain. Chem. Pharm.*, 2018, **10**, 97–102.
40 S. T. K. Narishetty and R. Panchagnula, *J. Contr. Release*, 2005, **102**, 59–70.
41 Z. Yang, L. Huang, X. Yao and H. Ji, *Flavour Fragr. J.*, 2017, **32**, 102–111.
42 F. Plati, R. Papi and A. Paraskevopoulou, *Foods*, 2021, **10**, 2923.
43 S. K. Kyasa, *J. Chem. Educ.*, 2020, **97**, 1966–1969.
44 Z. Triaux, H. Petitjean, E. Marchioni, M. Boltoeva and C. Marcic, *Anal. Bioanal. Chem.*, 2020, **412**, 933–948.
45 O. Shakil, F. Masood and T. Yasin, *Mater. Sci. Eng. C*, 2017, **77**, 173–183.
46 M. Farmahini-Farahani, A. Khan, P. Lu, A. H. Bedane, M. Eic and H. Xiao, *Appl. Clay Sci.*, 2017, **135**, 27–34.
47 K. J. Figueroa-Lopez, A. A. Vicente, M. A. M. Reis, S. Torres-Giner and J. M. Lagaron, *Nanomaterials*, 2019, **9**, 144.
48 S. M. B. Hashemi and A. M. Khaneghah, *Prog. Org. Coat.*, 2017, **110**, 35–41.
49 A. P. Lemes, T. L. A. Montanheiro, A. P. D. Silva and N. Durán, *J. Comput. Sci.*, 2019, **3**, 12.
50 M. N. Conceição, M. C. C. Santos, J. M. A. Mancipe, P. S. C. Pereira, R. C. C. Ribeiro, R. M. S. M. Thiré and D. C. Bastos, *Mater. Res.*, 2023, **26**, e20220615.
51 Y. Aoyagi, K. Yamashita and Y. Doi, *Polym. Degrad. Stab.*, 2002, **76**, 53–59.
52 J.-L. Audic, L. Lemiègre and Y.-M. Corre, *J. Appl. Polym. Sci.*, 2014, **131**, 1–7.
53 K. P. Menard, *Dynamic Mechanical Analysis - A Practical Introduction*, 1999.
54 S. Tunç, O. Duman and T. G. Polat, *Carbohydr. Polym.*, 2016, **150**, 259–268.
55 J. S. Choi and W. H. Park, *Polym. Test.*, 2004, **23**, 455–460.
56 P. D. Zygoura, E. K. Paleologos and M. G. Kontominas, *Radiat. Phys. Chem.*, 2011, **80**, 902–910.
57 P. Zhu, Y. Chen, J. Fang, Z. Wang, C. Xie, B. Hou, W. Chen and F. Xu, *J. Chem. Thermodyn.*, 2016, **92**, 198–206.

58 Y. Li, A. S. Fabiano-Tixier, C. Ginies and F. Chemat, *LWT–Food Sci. Technol.*, 2014, **59**, 724–731.
59 G. Amor, M. Sabbah, L. Caputo, M. Idbella, V. D. Feo, R. Porta, T. Fechtali and G. Mauriello, *Foods*, 2021, **10**, 121.
60 D. Garcia-Sotelo, B. Silva-Espinoza, M. Perez-Tello, I. Olivas, E. Alvarez-Parrilla, G. A. González-Aguilar and J. F. Ayala-Zavala, *LWT–Food Sci. Technol.*, 2019, **111**, 837–845.
61 J. H. Han, D. Patel, J. E. Kim and S. C. Min, *J. Food Sci.*, 2014, **79**, E2272–E2278.
62 G. S. Dannenberg, G. D. Funck, C. E. S. Cruxen, J. L. Marques, W. P. D. Silva and Â. M. Fiorentini, *LWT–Food Sci. Technol.*, 2017, **81**, 314–318.
63 M. C. Coelho, C. C. G. Silva, S. C. Ribeiro, M. L. N. E. Dapkevicius and H. J. D. Rosa, *Int. J. Food Microbiol.*, 2014, **191**, 53–59.